

of some tens of much smaller primary polymer particles 0.2–0.35  $\mu\text{m}$  in diameter, though these diameters may naturally vary, depending on the polymer yield and crystallite size.

At present the reason the secondary polymer globules are formed cannot be elucidated. To make this point clearer, we continue to make some additional studies.

**Registry No.**  $\text{OsO}_4$ , 20816-12-0;  $\text{MgCl}_2$ , 7786-30-3;  $\text{Al}(\text{C}_2\text{H}_5)_2\text{Cl}$ , 96-10-6;  $\text{Al}(\text{C}_2\text{H}_5)_3$ , 97-93-8;  $\text{TiCl}_3$ , 7705-07-9; polypropylene, 9003-07-0; 1,7-octadiene, 3710-30-3; methyl *p*-toluate, 99-75-2.

## References and Notes

- (1) Hock, C. W. *J. Polym. Sci., Polym. Chem. Ed.* **1966**, *4*, 3055–3064.
- (2) Buls, V. W.; Higgins, T. L. *J. Polym. Sci., Polym. Chem. Ed.* **1970**, *8*, 1037–1053.
- (3) Wilchinsky, Z. W.; Looney, R. W.; Tornqvist, E. G. M. *J. Catal.* **1973**, *28*, 351–367.
- (4) Murray, R. T.; Pearce, R.; Platt, D. *J. Polym. Sci., Polym. Lett. Ed.* **1978**, *16*, 303–308.
- (5) Barbe, P. C.; Cecchin, G.; Noristi, L. *Adv. Polym. Sci.* **1987**, *81*, 1–81.
- (6) Rodriguez, L. A. M.; Gabant, J. A. *J. Polym. Sci., C* **1963**, *4*, 125; *J. Polym. Sci., Polym. Chem. Ed.* **1966**, *4*, 1971–1992.
- (7) Blais, P.; John Manley, R. St. *J. Polym. Sci., Polym. Chem. Ed.* **1968**, *6*, 291–334.
- (8) Guttman, J. Y.; Guillet, J. E. *Macromolecules* **1968**, *1*, 461–463.
- (9) Keller, A.; Willmouth, F. M. *Makromol. Chem.* **1969**, *121*, 42–50.
- (10) Chanzy, H. D.; Marchessault, R. H. *Macromolecules* **1969**, *2*, 108–110.
- (11) Baker, R. T. K.; Harris, P. S.; Waite, R. J.; Roper, A. N. *J. Polym. Sci., Polym. Lett. Ed.* **1973**, *11*, 45–53.
- (12) Graff, R. J. L.; Kortleve, G.; Vonk, C. G. *J. Polym. Sci., Polym. Lett. Ed.* **1970**, *8*, 735–739.
- (13) Wristers, J. J. *J. Polym. Sci., Polym. Phys. Ed.* **1973**, *11*, 1601–1617.
- (14) Hoseman, R.; Hentschel, M.; Ferracini, E.; Ferrero, A.; Martelli, S.; Riva, F.; Vittori Antisari, M. *Polymer* **1982**, *23*, 979–984.
- (15) Mackie, P.; Berger, M. N.; Grieseson, B. M.; Lawson, D. J. *J. Polym. Sci., Polym. Lett. Ed.* **1967**, *5*, 493–494.
- (16) Kakugo, M.; Sadatoshi, H.; Yokoyama, M. *J. Polym. Sci., Polym. Lett. Ed.* **1986**, *24*, 171–175.
- (17) Warren, B. E.; Biscoe, J. *J. Am. Ceram. Soc.* **1938**, *21*, 49–54.
- (18) Natta, G.; Pasguon, I.; Giachetti, E. *Chim. Ind.* **1957**, *39*, 1002–1012.
- (19) Berney, C. V.; Cohen, R. E.; Bates, F. S. *Polymer* **1982**, *23*, 1222–1226.
- (20) Kakugo, M.; Sadatoshi, H.; Sakai, J.; Yokoyama, M. *Makromol. Chem.*, in press.
- (21)  $\delta\text{-TiCl}_3$  is shown by Guidetti et al.<sup>22</sup> to have the polymorphic form of  $\alpha$ - and  $\gamma\text{-TiCl}_3$ . In this study we describe the peak at  $2\theta = 51.5^\circ$  as (300) as a matter of convenience because  $\alpha\text{-TiCl}_3$  will be predominant in highly active  $\delta\text{-TiCl}_3$  as pointed out by them.
- (22) Guidetti, G.; Zannetti, R.; Ajo, D.; Marigo, A.; Vidali, M. *Eur. Polym. J.* **1980**, *16*, 1007–1015.

## Infrared and X-ray Diffraction Studies of a Semirigid Polyurethane

S. K. Pollack,<sup>†</sup> D. Y. Shen,<sup>†</sup> S. L. Hsu,<sup>\*,†</sup> Q. Wang,<sup>†</sup> and H. D. Stidham<sup>†</sup>

Department of Polymer Science and Engineering and Department of Chemistry, The University of Massachusetts, Amherst, Massachusetts 01003. Received May 9, 1988

**ABSTRACT:** A polyurethane containing a mesogenic diol has been studied by a combination of infrared spectroscopy and X-ray diffraction. Both techniques indicate that this polyurethane develops extremely high order/crystallinity upon annealing. Mid- and far-infrared studies indicate a variety of hydrogen-bonded environments exist in this polyurethane, even in the highly ordered state. In addition to the spectroscopic features arising from intermolecular interactions found for the carbonyl and N–H stretching vibrations, a band sensitive to chain packing and to temperature changes and found at approximately 105  $\text{cm}^{-1}$  can be assigned to hydrogen-bonded stretching between the N–H and the C=O groups. Infrared spectra change continuously with increasing temperature. However, only minor changes were observed at isotropization. Considerably different deuterium exchange rates found for urethane hydrogens also suggest different hydrogen bonds in this polyurethane. X-ray studies indicate that the mesophase is of a “cybotactic” nematic type and that the ordered/crystalline state may retain this kind of ordering.

## Introduction

Semirigid polymers represent an important and interesting class of materials. A great number of these systems have the potential for strongly ordered structure in the solid state and may have the possibility of exhibiting a liquid crystalline phase. In this study we have given emphasis to a class of semirigid polyurethanes. Unlike many other semirigid polymers, these polymers are strongly interacting. The principal goal in many previous studies has been to obtain a better understanding of the molecular features that allow for the development of the liquid crystalline state. However, most of the studies have concentrated on rigid or semirigid rod systems where the in-

teractions are limited to excluded volume effects and dispersive forces.<sup>1–3</sup> A large body of work exists detailing the effect of specific hydrogen-bonding interactions in polyurethane systems.<sup>4–10</sup> The system examined in this study has been shown to exhibit unique mechanical properties relative to more conventional flexible polyurethanes.<sup>11</sup> We would like to understand how the presence of the rigid regions and the hydrogen-bonding interactions in these polymers affect the ultimate structure and resultant properties.

We have been interested for some time in understanding the nature of phase transitions as they relate to the degree of order and disorder in polymeric systems. The microstructural changes in the various functionalities within a polymer that accompany phase transitions can have varying contributions to the overall process. At least two phase transitions have been observed for these new poly-

<sup>†</sup>Department of Polymer Science and Engineering.

<sup>\*</sup>Department of Chemistry.

urethanes in differential scanning calorimetric studies.<sup>11</sup> The high-temperature peak has been interpreted as consistent with the behavior expected for the liquid crystalline isotropic transition. Previous studies for similar materials exhibit unique changes in both entropy and enthalpy.<sup>1,12,13</sup> The orientational entropy contribution for aspherical molecules can have a dominant effect in the phase transition of such systems.<sup>14</sup> The rigid units in these rigid or semirigid polymers have the appropriate asymmetry to exhibit this effect.

The melt processing of rigid-rod polymers is quite difficult, owing to the high melting temperature. For the practical utilization of semirigid polymers, especially systems bearing thermally labile functionality, flexible units are incorporated into the structure to achieve a lower melting temperature. These will contribute to the conformational entropy of the system. Few studies can measure the structural changes that these diverse types of structures undergo separately. However, for materials which contain a variety of functionalities, it may be possible to examine the contributions of the individual molecular entities to the disordering process.

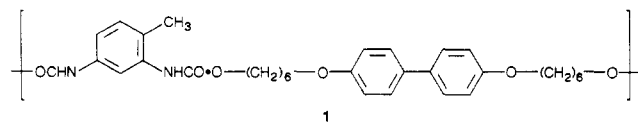
One of the principal techniques for examining chain-chain interaction and conformational order in these types of polymers is vibrational spectroscopy.<sup>15-17</sup> This method can be used to ascertain the degree of conformational order in flexible segments, the degree of self-association in the polyurethane linkages<sup>4-10</sup> and to assess other intra- and intermolecular interactions of the rigid aromatic units. For example, we have been able to determine the extent to which the disordering of aliphatic chains contributes to the overall entropy of phase transition versus the contribution of rigid aromatic groups in discotic liquid crystalline systems.<sup>18</sup> We have also examined how hydrogen-bonding interactions affect the structure of phase-separated domains in polyurethane systems.<sup>19</sup>

While vibrational spectroscopy provides a measure of localized structure, these are averaged over the entire sample and do not give a good measure of the long-range ordering effects of microstructural phenomena. X-ray diffraction techniques examine the long-range order produced as a consequence of very short-range interactions.<sup>1,20</sup> In combination, these two approaches provide a more complete picture of the overall effects of microstructure on the polymer morphology.

The bis(alkylidene)biphenol mesogen has been incorporated into a number of systems which have been shown to exhibit a mesogenic phase.<sup>21-25</sup> Urethane-based liquid crystalline polymers have been previously reported,<sup>26,27</sup> but the microstructural changes which accompany phase transitions were not studied. The polyurethane used in this study provides three unique functionalities. The hexamethylene sequences may give a measure of intramolecular disorder as measured by the *trans/gauche* ratio. The biphenol unit may be used to probe the nature of the intramolecular forces which produce ordering in the liquid crystalline phase. Finally the urethane linkage provides a probe of potentially strong intermolecular interaction due to hydrogen bonding. First results are reported here.

## Experimental Section

Samples of poly(4,4'-bis(6-hydroxyhexoxy)biphenyl 2,4-tolylene diisocyanate) (1) were provided to us by Stenhouse et al.



The synthesis and physical characterization are described else-

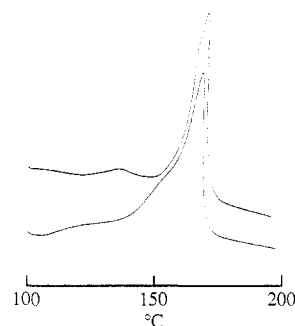


**Figure 1.** Differential scanning calorimetry (DSC) scans for 1 (heating rate 20 °C/min): upper trace, annealed 2 h at 150 °C; lower trace, annealed 15 min at 150 °C.

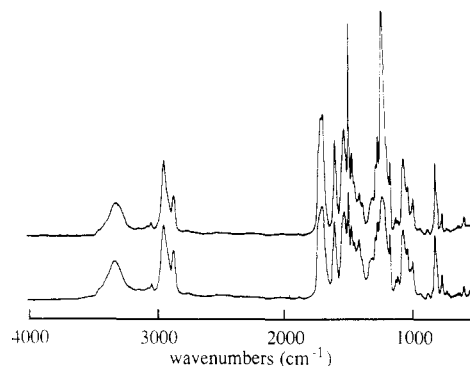


**Figure 2.** Mid-infrared spectra of 1: lower spectrum: no thermal treatment; upper spectrum, annealed at 150 °C for 2 h.

where.<sup>11</sup> Several transitions were observed in DSC. As shown in Figure 1 the exact temperatures of these transitions may be strongly dependent on thermal history.

Thin films for infrared studies were prepared either by solution casting or from the melt. For solution cast films, 1% (w/v) of 1 was dissolved in spectrograde DMF and poured onto glass plates and the solvent removed in vacuo. Complete removal of solvent was determined by disappearance of the DMF amide I band in the spectrum. Further thermal processing was done at this point, generally in vacuo. Attempts to generate oriented films from solution by casting on fresh cleaved mica surfaces as suggested by some workers<sup>1</sup> proved unsuccessful in this system.

Films of 100–300  $\mu\text{m}$  in thickness suitable for far-infrared studies were pressed from precipitated polymer at 190 °C ( $T_i = 172$  °C). These films were cooled in the press. In addition films were prepared by melting precipitated polymer between poly-(tetrafluoroethylene) sheets—the molten polymer was sheared to achieve the desired thickness and then quenched in ice water to minimize crystallization. These films were oriented by stretching to 300% strain in a stretcher at just below  $T_g$  (95 °C). Further thermal processing was done at this point.

Infrared spectra were obtained utilizing either an IBM Model 32 or Bruker IFS 113V Fourier transform infrared spectrometer. In both cases, 2  $\text{cm}^{-1}$  resolution spectra were collected and then transferred to an IBM CS9000 computer for further analysis. All spectra were collected in the transmission mode either of free standing films or of films held between KBr windows. High-temperature studies were performed with films held between KBr windows in a cell described previously.<sup>19</sup> The sample temperature was measured at the window. All polarization studies were performed on the Bruker IFS 113V with a Genzel interferometer to minimize inherent polarization due to the spectrometer. A wire grid polarizer mounted after the sample was used to achieve linear polarization of the infrared radiation. Far-infrared data were obtained with the Bruker evacuable instrument. The infrared spectra obtained for samples with different thermal history are shown in Figures 2–4. The changes in the infrared data as a function of temperature are shown in Figures 5 and 6. Because of the complexity associated with the NH stretching vibration, quantitative structural information is usually not readily obtained. However, changes can be observed and are shown in Figures 7 and 8.

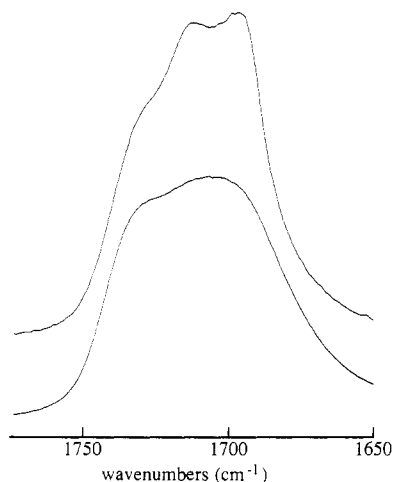


**Figure 3.** Carbonyl stretching region of 1: lower spectrum, no thermal treatment; upper spectrum, annealed at 150 °C for 2 h.

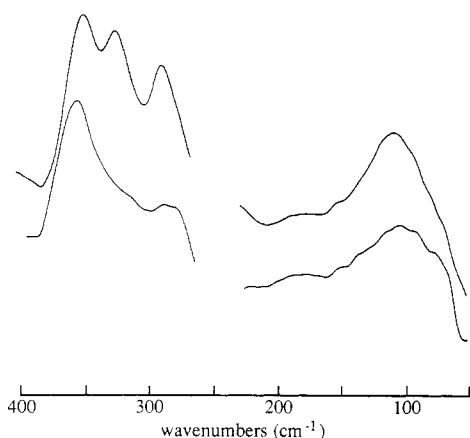


**Figure 4.** Far-IR spectra of 1: lower spectrum, no thermal treatment; upper spectrum, annealed at 150 °C for 2 h.

X-ray diffraction photographs were obtained utilizing a Statton Camera with Ni-filtered Cu K $\alpha$  radiation. All diffraction data were obtained at room temperature with sample films mounted directly on the pin hole.

## Results and Discussion

Figure 1 shows differential scanning calorimetric (DSC) traces of 1 with different annealing histories. The high-temperature transition ( $T = 172$  °C), which we will refer to as the isotropization transition ( $T_i$ ), is unaffected by the thermal history of the sample. The lower temperature transition, which we will refer to as the melting transition ( $T_m$ ), is highly sensitive to annealing conditions. This sort of behavior has been observed in a number of liquid crystalline polymers.<sup>2,28,29</sup> The thermal history also has a profound effect on the temperature-induced changes in the vibrational spectrum of this polymer.

An infrared spectrum of 1 is shown in Figure 2. The main features include the NH stretch in the 3500–3200  $\text{cm}^{-1}$  region, the carbonyl stretch in the 1735–1699  $\text{cm}^{-1}$  region and the fingerprint region below 1600  $\text{cm}^{-1}$ . The first two regions are discussed in some detail below.

Perhaps the most readily discerned change in the fingerprint region upon annealing is the appearance of the relatively weak bands at 1470 and 1430  $\text{cm}^{-1}$  and the considerable intensifications of the aromatic band near 1500  $\text{cm}^{-1}$  and the broad feature near 1250  $\text{cm}^{-1}$ . A number of bands that exhibit intensity changes or frequency shifts on annealing and for which secure assignments to vibrational modes can be made are collected in Table I. Other bands in this region are of uncertain origin, and it is dif-

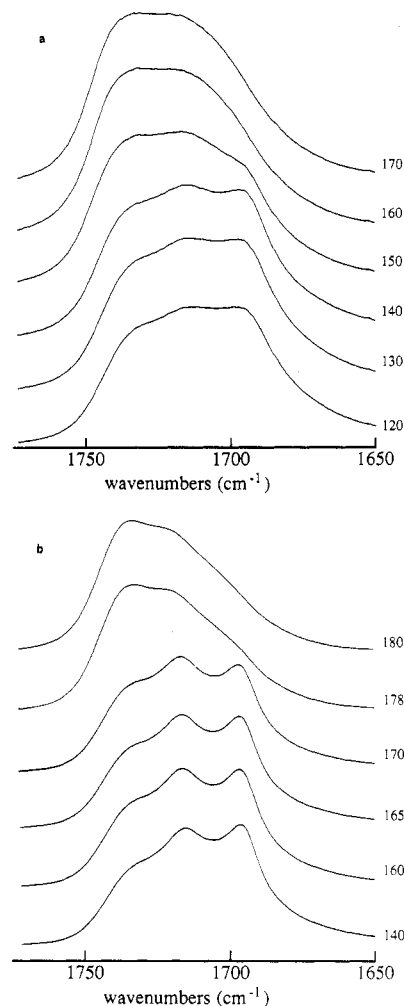


**Figure 5.** Carbonyl stretching region of 1 as a function of temperature: (a) no thermal treatment; (b) annealed at 150 °C for 2 h. Temperatures are in °C.

**Table I**  
Frequency Shifts Due to Annealing<sup>a</sup>

$\nu(\text{unannealed})$	$\nu(\text{annealed})$	assignment
1731	1735	free C=O stretch
1707	1714/1695	H-bonded C=O stretch
1607	1603	ring C—C stretch
1537	1534	amide II
1502	1499	ring C—C stretch
1418	1415	ring C—C stretch
1176	1173	CH in-plane bend
733	728	CH <sub>2</sub> rock

<sup>a</sup> Frequency values in  $\text{cm}^{-1}$ .

ficult to utilize them for structural characterization.

The most easily interpretable bands in this system are due to the C=O stretching or the N—H stretching vibrations. It has been known for some time that the frequencies and relative intensities of these vibrations are characteristic of hydrogen-bond formation. This is particularly so for the N—H stretching vibration. In the carbonyl region (Figure 3), in unannealed samples, we observe a shoulder at 1735  $\text{cm}^{-1}$ , typically assigned to free (non-hydrogen-bonded) urethane carbonyls.<sup>9,19</sup> There is also a broad band, centered at 1708  $\text{cm}^{-1}$ . The breadth and position of the absorption suggest it may be due to a distribution of carbonyls with differing hydrogen-bonded geometries. This band has also been observed for other 2,4-TDI based amorphous polyurethanes and has been ascribed to the hydrogen-bonded carbonyl component.<sup>7</sup> Upon annealing, a significant change occurs, with relatively

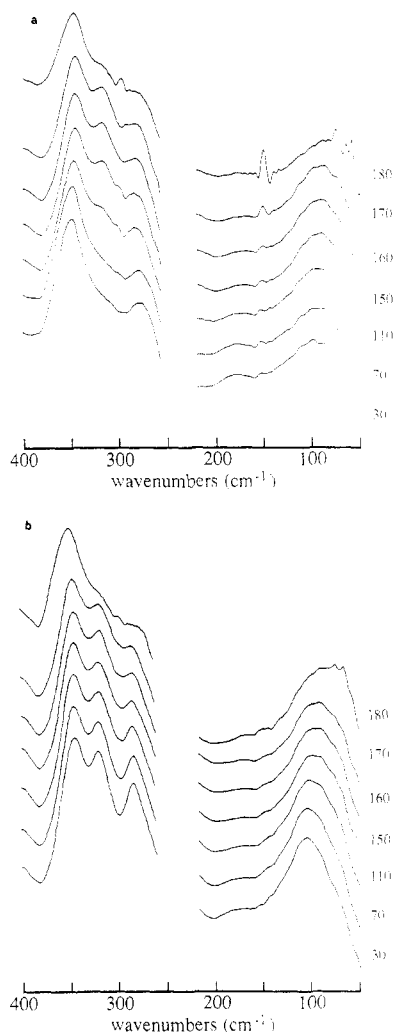


**Figure 6.** Far-IR spectra of 1 as a function of temperature: (a) no thermal treatment; (b) annealed at 150 °C for 2 h. Temperatures are in °C.

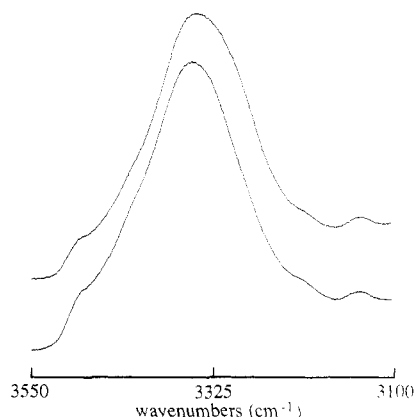


**Figure 7.** NH stretching region of 1: lower spectrum, no thermal treatment; upper spectrum, annealed at 150 °C for 2 h.

sharp bands at 1699 and 1714  $\text{cm}^{-1}$  becoming evident. While the 1699  $\text{cm}^{-1}$  band may be assigned confidently to hydrogen-bonded carbonyl,<sup>10,19</sup> the intermediate frequency value for the 1714  $\text{cm}^{-1}$  band allows several alternative explanations, one of which is an uniquely different hydrogen bonding geometry. Other investigators have also observed carbonyl bands at frequencies between the free and ordered hydrogen-bonded limits and have ascribed them to irregularly H-bonded carbonyls<sup>9,30</sup> or as possibly due to transition dipole-dipole coupling in highly ordered structures.<sup>31</sup>

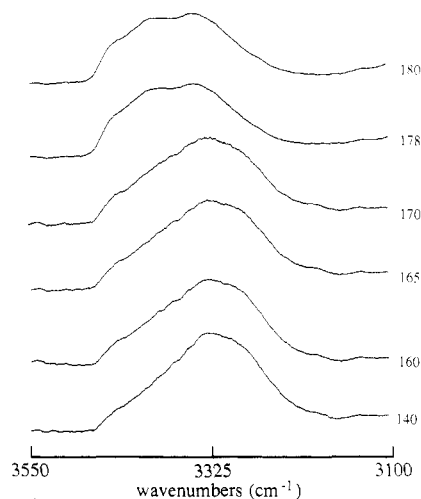


**Figure 8.** NH stretching region of annealed sample (2 h at 150 °C) of 1 as a function of temperature. Temperatures are in °C.

On the basis of the DSC results presented above, it is tempting to ascribe the spectroscopic changes we observed to the introduction of a crystalline phase. To confirm this, annealed samples were examined as a function of temperature. Samples with annealing histories exhibit a discontinuous change in the infrared spectrum as a function of heating. While changes are observed throughout the spectrum, the most readily discerned affects are observed in the carbonyl region (Figure 5). In the less well-annealed sample, the spectrum exhibits a change at 150 °C. In the well-annealed sample the same sort of spectroscopic change occurs above 170 °C, very close to the isotropization transition ( $T_i = 172$  °C). In both cases, after this abrupt change, the overall spectrum exhibits only slight changes in this region above this temperature, with a gradual decrease in the hydrogen-bonded carbonyl and a corresponding increase in the 1735  $\text{cm}^{-1}$  band, due to the free carbonyl. This result suggested careful examination of DSC scans for materials with similar annealing histories to those of the samples above. Extensive annealing shifted the melting transition to higher temperatures which caused it nearly to overlap the isotropization transition (Figure 1). This led to the interpretation that the abrupt changes observed in spectra of samples with both types of annealing histories are due to the removal of crystalline order and that only gradual changes occur upon isotropization. This type of behavior has also been observed in a number of liquid crystalline polymers.<sup>16</sup> Attempts to assign bands present in the three phases to ordered or disordered bands of the methylene sequences proved unsuccessful, due to interference from strongly overlapping aromatic ring modes and vibrations due to the urethane linkage.<sup>7</sup>

Another potential region for study contains the N-H stretching vibrations, from 3500 to 3200  $\text{cm}^{-1}$ . Changes in the region as a result of thermal annealing have been examined by others,<sup>7</sup> and the appearance of new bands at lower frequencies is thought to be indicative of the development of an extremely high degree of order. One does in fact observe a shoulder at lower frequency (Figure 7) which would be due to stronger and more specific hydrogen bonding than present in the unannealed case. To determine if this new band was due to more crystalline regions, we exchanged the annealed samples with deuterium oxide at 70 °C for 12 h. Figure 9 shows spectra before and after exchanging N-H for N-D. There is a distinct decrease in the band at 3323  $\text{cm}^{-1}$  while the low-frequency shoulder has resolved into a well-defined band centered at 3281  $\text{cm}^{-1}$ . The fact that the exchange rates for these different

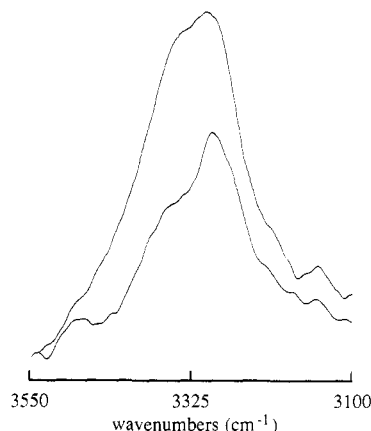


**Figure 9.** Effects of deuterium exchange on NH stretch region: upper spectrum, prior to exchange; lower spectrum, after exchange as per text.

hydrogen-bonded bands is quite different implies a difference in diffusion rates and/or in the accessibility of the amide NH groups in the highly ordered crystalline regions versus less ordered amorphous states.<sup>32-34</sup> Exchange using ethanol-*d*<sub>1</sub> proceeded more rapidly at room temperature but produced the same changes in the spectrum as observed in deuterium oxide exchange. It should be emphasized that the relative heights of these bands are different but do not necessarily reflect the amount of each H-bonding environment, as the intensity of the N-H stretching vibration is a strong function of H-bonding strength.<sup>35</sup>

The presence of crystallinity in polyurethanes based on 2,4-toluene diisocyanate is very unusual.<sup>4,7</sup> Reactivity of the two isocyanate groups is such that one would anticipate a relatively random distribution. Thus, the structure shown as 1 should also have the methyl group adjacent to the other urethane linkage at random sites along the polymer chain. This disorder tends to inhibit crystallinity in conventional 2,4-TDI based polymers. In contrast 2,6-TDI based polyurethanes do tend to crystallize.<sup>7</sup> Certain liquid crystalline polyesters based on terephthalic acid and monosubstituted dihydroxyquinones have been observed to exhibit crystallinity, despite the potential for random orientation of the substituent along the chain.<sup>36</sup> The presence of crystallinity in 1 strongly suggests a dominant interaction of the mesogenic biphenol units, inducing the formation of crystalline phases. One possible consequence of this is that the remainder of the molecule may be forced to assume higher energy local conformations to allow for packing of the mesogenic units. This could explain the fact that after annealing the 1708 cm<sup>-1</sup> band splits into two components, one at 1714 cm<sup>-1</sup> and one at 1699 cm<sup>-1</sup>. The packing of the crystalline phase might allow for one relatively strong hydrogen bond. The other may be forced into a less than ideal hydrogen bonding geometry. This hypothesis is discussed with the X-ray diffraction results.

The far-IR region is sensitive both to chain packing and to hydrogen-bonding geometry. This extremely low-frequency region (300–10 cm<sup>-1</sup>) is usually difficult to study because most polymer samples lack sufficient order to define a unique hydrogen-bonding bending or heavy-atom stretching vibration. Previous successful far-infrared studies have assigned the heavy-atom stretching modes of the hydrogen bonds in the 250–50 cm<sup>-1</sup> region;<sup>37</sup> most are observed between 100 and 180 cm<sup>-1</sup>.<sup>38</sup> From normal-coordinate vibrational analysis of crystalline polyglycine I, the heavy atom stretching mode of the hydrogen bond in the unit cell is located in the 150–100 cm<sup>-1</sup> region.<sup>39</sup> Frank

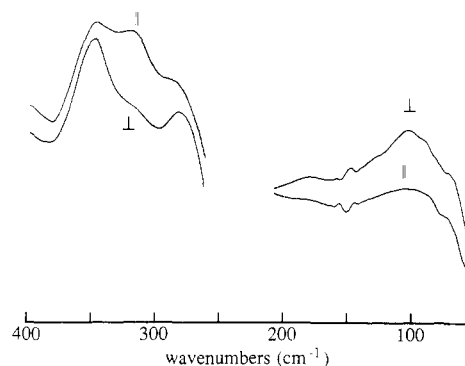


**Figure 10.** Infrared dichroism of far-IR active bands of 1 (polarizations as indicated).

et al.<sup>40</sup> have examined homologous series of polyamides (Nylon 2, 4, 6, 8, 10, and 12) in the far-infrared region and found that a common property of all spectra is a band between 100 and 110 cm<sup>-1</sup> (except for polyglycine in which a band appears at 116 cm<sup>-1</sup>) which seems to be independent of chain conformation. They proposed a simple vibrational model of hydrogen-bonding stretching and assigned the observed band in all the polyamide spectra to a translational vibration of the amide group. If the amide group is rigid and can move as a whole under the influence of the hydrogen-bond force constant, the frequency of the heavy-atom hydrogen-bond stretching mode can be estimated by

$$\nu_{O\cdots N} = 130.3(f_2/2M)^{1/2} \text{ cm}^{-1}$$

with reduced mass  $M$ , where  $M = m_C + m_O + m_N + m_H$ . In their system the value of  $M$  is 43 amu. From the bonded and nonbonded N-H group frequencies reported, the force constant of the hydrogen bond was calculated to be  $f_2 = 56 \text{ N/m}$  to yield  $\nu_{O\cdots N} = 105 \text{ cm}^{-1}$ .<sup>40</sup>

Figure 4 shows the band at 101 cm<sup>-1</sup> for amorphous samples shifts to 107 cm<sup>-1</sup> for the more crystalline sample. This fact indicated that this band is sensitive to packing structure of the samples. If this is actually a hydrogen-bond stretching vibration, according to Frank's model the average force constant of the hydrogen bonding is 52 N/m for amorphous sample and 58 N/m for the more crystalline sample, respectively, consistent with our expectations. In the crystalline state, if there are two unique hydrogen-bonding geometries, we might anticipate observing two low-frequency modes. Due to the signal to noise ratio in this region of the spectrum, we were unable to resolve more than the single broad band. The low-frequency hydrogen bond stretching vibration band is very sensitive to temperature change. It should be noted, however, the virtually all bands sensitive to the specificity and magnitude of nonbonded intermolecular interactions exhibit strong dependence on temperature changes. At low temperature (–77 °C) the sample is denser and the band shifts to 115 cm<sup>-1</sup>. As Figure 6 shows, when the sample melts, the band does not disappear but shifts to lower frequency (88 cm<sup>-1</sup>). Figure 10 shows the polarized far-infrared spectrum of amorphous polyurethane at 300% elongation (stretched at 85 °C, draw rate is 600%/min). Drawing the sample will tend to cause a net alignment of the polymer backbone in the draw direction. This will orient the interchain hydrogen bonds perpendicular to the draw direction. Our polarized infrared data indicated that the band around 105 cm<sup>-1</sup> has perpendicular dichroism and that coincides with the assignment of hydrogen-bonded band.

The X-ray diffraction pattern for a single fiber pulled from the melt and quenched in air is shown in Figure 11. The pattern exhibits equatorial reflections corresponding

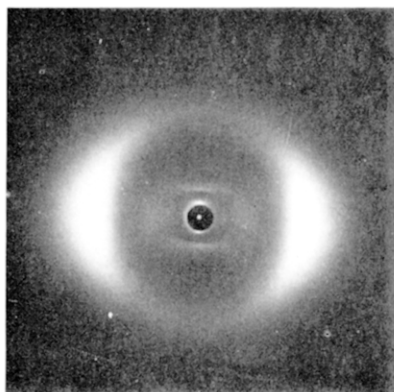


**Figure 11.** Room-temperature X-ray diffraction pattern from single fiber of 1 drawn from melt (sample to film distance 53.1 mm; exposure time 20 h). Draw axis is oriented vertically.

to a spacing of 4.5 Å. In addition one can observe off-meridional reflections. These types of patterns have been observed for a number of main-chain liquid crystalline polymers<sup>1,20,41</sup> and have been attributed to the so-called "cybotactic" nematic structure, involving a regular skewing of the mesogenic units between chains (having a smectic C-like structure).<sup>20,42</sup> The spacing of the innermost, off-meridional reflections correspond to a repeat of approximately 30 Å. This corresponds to a nearly extended monomeric unit. The structure is also present in the diffraction patterns of unannealed oriented films (Figure 12a). In this case, the inner off-meridional reflections are clearly visible, and the spacings are the same as found in Figure 11. Upon annealing, dramatic changes occur in the overall diffraction pattern (Figure 12b). The diffuse off-meridional reflections have sharpened into strong reflections, with the innermost reflection corresponding to a spacing of 30.1 Å. The outer reflections have resolved into two equatorial reflections with spacing corresponding to 4.0 and 4.75 Å. There are also a number of high-angle equatorial reflections present as well as several new reflections present off-meridional.

The relative intensities of the innermost reflections are unusual and deserve some discussion. Polymer 1 has two electron-rich units, the biphenyl and the 2,4-TDI. The biphenyl is situated halfway between each pair of 2,4-TDI

units (or vice versa). In the extended chain, these two units will have roughly identical spacings, so that the first-order reflections from the two repeats may interfere, reducing its intensity relative to the higher order reflection.<sup>43</sup> In earlier work on crystalline polyurethane systems, based on methylenediphenyl diisocyanate (MDI),<sup>44</sup> the same type of intensity in the off-meridional reflections were observed. These systems were also interpreted as having a skewed packing structure.

We were unable to obtain intensity data for Figure 12b, so a full structure refinement was not attempted. Using spacing for the innermost reflection to represent the length of the repeat in the triclinic unit cell (estimated to have a geometry of  $a = 4.9$  Å,  $b = 7$  Å,  $c = 29.9$  Å,  $\alpha = 95^\circ$ ,  $\beta = 105.4^\circ$ ,  $\gamma = 90^\circ$ ) we have utilized an interactive molecular modeling system to generate a conformation consistent with the derived dimensions. This structure (Figure 13) allows for the ready formation of two distinct hydrogen bonding geometries in the crystalline state (Figure 14), one with a favorable linear geometry and one of bent geometry. The perspective of this drawing somewhat exaggerates the difference in H-bond geometries. Calculated values from this dimer structure give bond lengths of 1.29 and 1.40 Å. The shorter bond has NH...O and H...OC angles of  $171^\circ$  and  $172^\circ$ , respectively, the same angles in the longer bond being  $163^\circ$  and  $161^\circ$ , respectively. The carbonyl vibration for the shorter bond should correspond to the  $1699\text{ cm}^{-1}$  band and that of the longer bond correspond to the band at  $1714\text{ cm}^{-1}$ .

### Conclusions

The mesogen-containing polyurethane examined in this study has been shown to exhibit X-ray patterns indicating the likely presence of a mesophase in melt-processed fibers and oriented films. Further thermal processing readily converts this mesophase into an ordered crystalline phase which reflects the underlying order of the liquid crystalline state. The crystalline state exhibits unique hydrogen-bonded structures which involve H bonds of two different geometries. This is reflected in the mid- and far-infrared data and in the proposed crystalline packing. The presence of both the melting and isotropization transitions suggests the coexistence of both a crystalline state and a less ordered mesophase in the solid state upon annealing. This

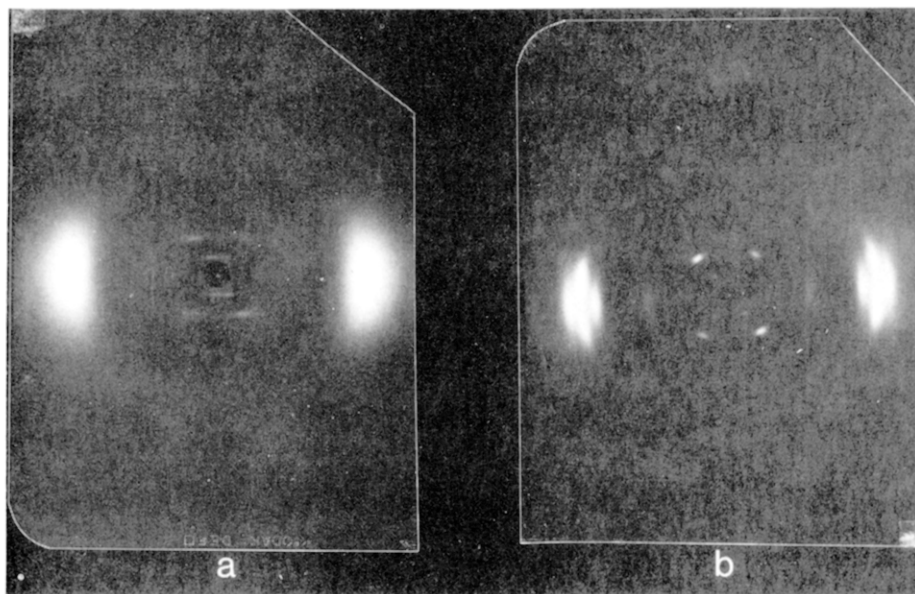


**Figure 12.** Room-temperature X-ray diffraction pattern of films of 1: (a) sheared from melt, then oriented by stretching to 300% elongation at 80–90 °C; (b) prepared as in Figure 12a, then annealed for 2 h at 150 °C (sample to film distance 75.2 mm; exposure time 4 h). Draw axis oriented vertically.

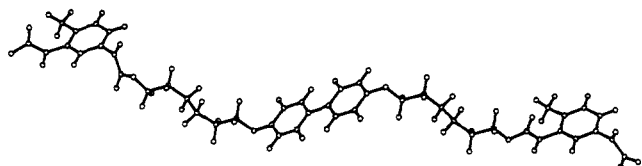


**Figure 13.** Model structure of monomer unit of 1 (plus next 2,4-TDI unit); repeat length is 32 Å.

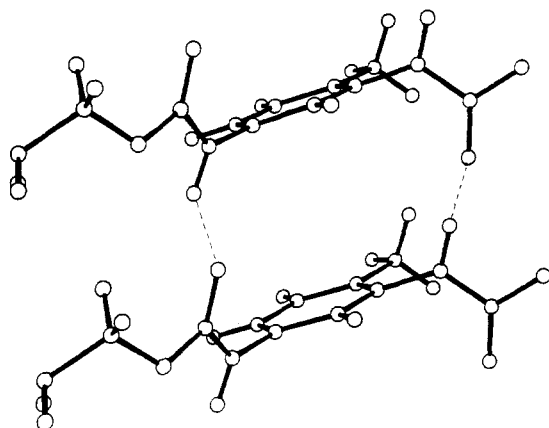


**Figure 14.** Schematic drawing showing the hydrogen bonds between a pair of 1 monomer units.

may be due to the relatively broad molecular weight distribution generated during the thermal processing of this material.<sup>11</sup> The lack of clear spectral change in the isotropization of 1 tends to indicate that only minor conformational changes are involved and changes in relatively weak intramolecular interactions not readily measured in the mid-infrared occur during this phase transition. Finally this study shows the complementarity of the microstructural information gained from spectroscopic studies and the more macroscopic perspective given by X-ray diffraction studies.

**Acknowledgment.** We thank Professor Simon Kantor and Mr. Peter Stenhouse for providing samples of the polymer. Additionally, we thank Professor E. D. T. Atkins for useful discussions on the interpretation of our X-ray results. We wish to thank Dr. Judith Kelley of the University of Connecticut for use of their Evans & Sutherland Graphics system. This research has been supported by a grant from the Army Research Office, ARO 23941-CH, and by the NSF US-China Cooperative Research Grant INT-8713724.

**Registry No.** 1 (copolymer), 117252-65-0; 2 (SRU), 117308-04-0.

## References and Notes

- (1) Noël, C. In *Recent Advances in Liquid Crystalline Polymers*; Chapoy, L. L., Ed.; Elsevier: Amsterdam, 1985.
- (2) Koide, N. *Mol. Cryst. Liq. Cryst.* **1986**, *139*, 47.
- (3) Finkelmann, H. *Angew. Chem. Int. Ed. Engl.* **1987**, *26*, 816.
- (4) MacKnight, W. J.; Yang, M. *J. Polym. Sci., Polym. Symp.* **1973**, *42*, 817.
- (5) West, J. C.; Cooper, S. L. *J. Polym. Sci., Polym. Symp.* **1977**, *60*, 127.
- (6) Koberstein, J. T.; Gancarz, I.; Clark, T. C. *J. Polym. Sci., Polym. Phys. Ed.* **1986**, *24*, 2487.
- (7) Brunette, C. M.; Hsu, S. L.; MacKnight, W. J. *Macromolecules* **1982**, *15*, 71.
- (8) Christenson, C. P.; Harthcock, M. A.; Meadows, M. D.; Spell, H. L.; Howard, W. L.; Crestwick, M. W.; Guerra, R. E.; Turner, R. B. *J. Polym. Sci., Polym. Phys. Ed.*; **1986**, *24*, 1401.
- (9) Coleman, M. M.; Lee, K. H.; Skrovanek, D. J.; Painter, P. C. *Macromolecules* **1986**, *19*, 2149.
- (10) Seymour, R. W.; Estes, G. M.; Cooper, S. L. *Macromolecules* **1970**, *3*, 579.
- (11) Stenhouse, P. J.; Valles, E. M.; Kantor, S. W.; Mac Knight, W. J. *Macromolecules*, in press.
- (12) Griffin, A. C.; Haven, S. J. *J. Polym. Sci., Polym. Phys. Ed.* **1981**, *19*, 951.
- (13) Frosini, V.; de Petris, S.; Chiellini, E.; Galli, G.; Lenz, R. W. *Mol. Cryst. Liq. Cryst.* **1983**, *98*, 223.
- (14) Flory, P. J.; Ronca, G. *Mol. Cryst. Liq. Cryst.* **1979**, *54*, 289.
- (15) Wu, P. P.; Hsu, S. L.; Thomas, O.; Blumstein, A. J. *Polym. Sci., Polym. Phys. Ed.* **1986**, *24*, 827.
- (16) Shibaev, V. P.; Platé, N. A.; Smolyansky, A. L.; Volloskov, A. Y. *Makromol. Chem.* **1980**, *181*, 1393.
- (17) Landreth, B. M.; Stupp, S. I. *Appl. Spectrosc.* **1986**, *40*, 1032.
- (18) Yang, X.; Kardan, M.; Hsu, S. L.; Collard, D.; Heath, R. B.; Lillya, C. P. *J. Phys. Chem.* **1988**, *92*, 196.
- (19) Lee, H. S.; Wang, Y. K.; MacKnight, W. J.; Hsu, S. L. *Macromolecules* **1988**, *21*, 270.
- (20) Azaroff, L. V. *Mol. Cryst. Liq. Cryst.* **1987**, *145*, 31.
- (21) Sato, M.; Nakatsuchi, K.; Ohkatsu, Y. *Makromol. Chem., Rapid Commun.* **1986**, *7*, 231.
- (22) Shaffer, T. D.; Percec, V. *J. Polym. Sci., Polym. Lett. Ed.* **1985**, *23*, 185.
- (23) Shaffer, T. D.; Jamaludin, M.; Percec, V. *J. Polym. Sci., Polym. Chem. Ed.* **1985**, *23*, 2913.
- (24) Blumstein, A.; Sivaramakrishnan, K. N.; Clough, S. B.; Blumstein, R. B. *Mol. Cryst. Liq. Cryst.* **1979**, *49*, 255.
- (25) Shaffer, T. D.; Percec, V. *Makromol. Chem.* **1986**, *187*, 111.
- (26) Iimura, K.; Koide, N.; Tanabe, H.; Takeda, M. *Makromol. Chem.* **1981**, *182*, 2569.
- (27) Tanaka, M.; Nakaya, T. *J. Macromol. Sci., Chem.* **1987**, *A24*, 777.
- (28) Galli, G.; Genedetti, E.; Chiellini, E.; Obert, C.; Lenz, R. W. *Polym. Bull.* **1981**, *5*, 497.
- (29) Noël, C.; Friedrich, C.; Bosio, L.; Strazielle, C. *Polymer* **1984**, *25*, 1281.
- (30) Walters, G.; Painter, P.; Ika, P.; Frisch, H. *Macromolecules* **1986**, *19*, 888.
- (31) Moore, W. H.; Krimm, S. *Proc. Natl. Acad. Sci. U.S.A.* **1979**, *72*, 4933.
- (32) Nakanishi, M.; Tsuboi, M.; Ikegami, A.; Kanehisa, M. *J. Mol. Biol.* **1972**, *64*, 363.
- (33) Seilser, H. W.; Holland-Moritz, K. *Infrared and Raman Spectroscopy of Polymers*; Marcel Dekker: New York, 1980; pp 292-307.
- (34) Tadokoro, H. *Structure of Crystalline Polymers*; Wiley-Interscience: New York, 1979; pp 199-203.
- (35) Tsubomura, H. *J. Chem. Phys.* **1956**, *24*, 927.
- (36) Blackwell, J.; Biswas, A. *Polym. Prepr.* **1988**, *29*(1), 474.
- (37) Pimental, G. C.; McClelland, A. L. *The Hydrogen Bond*; Reinhold: New York, 1960.
- (38) Moler, K. D.; Rothschild, W. G. *Far Infrared Spectroscopy*; Wiley-Interscience: New York, 1971; p 198.
- (39) Moore, K. D.; Krimm, S. *Biopolymers* **1976**, *15*, 2439.
- (40) Frank, W. F. X.; Fielder, H. *Infrared Phys.* **1979**, *19*, 481(1979).
- (41) Blumstein, A.; Thomas, O.; Asrar, J.; Makris, P.; Clough, S. B.; Blumstein, R. B. *J. Polym. Sci., Polym. Lett. Ed.* **1984**, *22*, 13.
- (42) Roviello, A.; Sirigu, A. *Eur. Polym. J.* **1979**, *15*, 61.
- (43) Atkins, E. D. T., private communications.
- (44) Blackwell, J.; Nagarjan, M. R.; Hoitink, T. B. *Polymer* **1982**, *23*, 950.